Structural Engineering and Mechanics, Vol. 18, No. 6 (2004) 769-790
DOI: http://dx.doi.org/10.12989/sem.2004.18.6.769

Strength and strain enhancements of concrete columns confined with FRP sheets

G. Campione†, N. Miraglia‡ and M. Papia‡†

Dipartimento di Ingegneria Strutturale e Geotecnica, Università di Palermo
Viale delle Scienze – 90128 Palermo, Italy

(Received March 12, 2004, Accepted July 23, 2004)

Abstract. The compressive behavior up to failure of short concrete members reinforced with fiber reinforced plastic (FRP) is investigated. Rectangular cross-sections are analysed by means of a simplified elastic model, able also to explain stress-concentration. The model allows one to evaluate the equivalent uniform confining pressure in ultimate conditions referred to the effective confined cross-section and to the effective stresses in FRP along the sides of section; consequently, it makes it possible to determine ultimate strain and the related bearing capacity of the confined member corresponding to FRP failure. The effect of local reinforcements constitute by single strips applied at corners before the continuous wrapping and the effect of round corners are also considered. Analytical results are compared to experimental values available in the literature.

Key words: FRP; confinement; rectangular cross-section; stress-concentration; maximum compressive strength; ultimate strain.

1. Introduction

Fiber reinforced plastic (FRP) materials are very often utilised in the form of bars, strips or sheets for retrofitting or strengthening of reinforced concrete members subjected mainly to axial or flexural and shear forces. In the case of RC columns the most common use of these materials is based on external wrapping with flexible layers of FRP sheets. The connection of FRP sheets to reinforced concrete members proves to be effective with epoxy resin and adopting adequate over-lap length obtained by wrapping the FRP on itself. This reinforcing technique can determine enhancements of strength and strain capacities due to the lateral restraint (confinement effect) exercised by FRP.

Many well documented experimental and analytical studies refer to this subject (Saadatmanesh *et al.* 1997, Mirmiran *et al.* 1998, Demers and Neale 1999, Purba and Mufti 1999, Saafi *et al.* 1999, Spoelstra and Monti 1999, Toutanji 1999, Rochette and Labossiére 2000, Campione *et al.* 2001, Shehata *et al.* 2002, Ilki and Kumbasar 2002, Moran and Pantalides 2002, Tan 2002, Chaallal *et al.* 2003, Campione and Miraglia 2003, Maalej *et al.* 2003). These studies mainly show that the choice of the type of reinforcing material (glass, aramid, carbon, etc.) and of the number of layers depends

† Associate Professor
‡ Assistant Professor
‡† Full Professor and Dean of the Department

on several factors, such as: - increase in compressive strength required by the structural members; - grade of concrete; - shape and size of members to be wrapped, etc.

In the case of wrapping concrete members with thin layers of FRP, unlike what occurs using transverse steel reinforcement, it can be assumed that the confinement effect is continuous all along the length of the member. Moreover, due to the poor flexural stiffness of the FRP package, low average transverse confining pressure can be exercised in square and rectangular cross-sections. At the sharp corners of these sections the high axial and the low flexural stiffness of the FRP package produces dangerous stress concentrations up to concrete failure occurring when the stress in the fibers along the perimeter of the section is still much lower than the ultimate strength value and strain-softening behavior of confined concrete is observed (Mirmiram *et al.* 1998).

CEB-FIP recommendations (CEB-FIP 2001) highlight this problem and suggest reducing stress concentration by smoothing the sharp corners with round fillets before the application of FRP reinforcing layers. Moreover, CEB-FIP advises against utilising FRP when the rectangular transverse cross-section is extended. Some researches propose using FRP for extended rectangular cross-sections by inserting transversally adequate connection elements (La Tegola and Manni 1998) while more recently it has been proposed transforming the shape of the section from rectangular to elliptical (CEB-FIP 2001, Teng and Lam 2002).

The implementation of round corners in square or rectangular cross-sections before the application of a continuous FRP layer involves additional costs and often cannot be done (e.g., when a reduced cover is present in a reinforced concrete member). In these cases the use of single strips of FRP locally applied at the sharp corners before the continuous wrapping of the transverse cross-section should be a good alternative technique, able to avoid premature collapse due to local stress peaks in the FRP sheets (Campione *et al.* 2003).

This paper originates form the opportuneness of interpreting the effectiveness of this technique by an analytical approach, simple enough that it can be utilised for practical applications. Obviously, the analytical model which is proposed here concerns the more general problem of predicting the compressive behavior of concrete members having different cross-sectional shapes. Its ability to quantify the improvement effects of FRP sheets locally applied at the corners of rectangular sections merely confirms the reliability of the proposed approach to represent the confinement mechanism in this particular case too.

2. Simplified model of confinement effect

To explain in a simplified way the confinement effects in the concrete core due to the presence by FRP wraps, which can be pointed out numerically by a finite element approach, a simplified analysis is carried out. It refers to the geometrical model shown in Fig. 1, representing a three dimensional prismatic concrete member having cross-section of side L and wrapped with FRP sheets. The continuous FRP wrap is assumed to be externally applied to the concrete surface with an adequate overlap length. If the concrete member is loaded axially, and maintains its prismatic shape, it tends to be subjected to an axial strain ε_v and a lateral strain $\varepsilon = \nu_c \times \varepsilon_v$, ($\nu_c$ being the elastic Poisson coefficient of the concrete core) that are partially reduced by the presence of the FRP sheet. A fictitious lateral strain ε_1 produces confinement pressures resulting an effective lateral strain $\varepsilon_{eff} = \varepsilon - \varepsilon_1$.

Because of the adhesion between concrete surface and FRP sheets, shear stress distribution arises

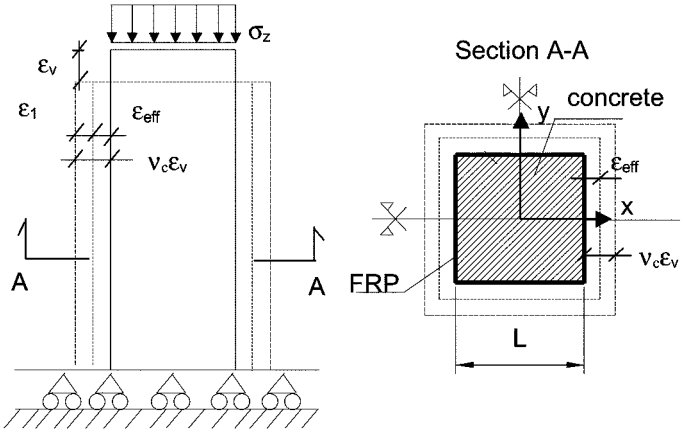

Fig. 1 Geometrical model for FRP wrapped prismatic specimens

at the interfaces, with intensification of axial stresses in the fibers close to the corners of the cross-section. Moreover, the interaction between FRP and concrete core produces confinement pressure in the direction perpendicular to the fiber, with non uniform distribution and maximum values at the corners.

In the following only confinement pressures will be considered, while shear stresses will be neglected assuming that when concrete reaches maximum compressive strength complete detachment between concrete interface and FRP package occurs as shown in Mirmiran *et al.* (1998) and increases in maximum strength is due only to confinement pressures.

In the case of a compressed member having rectangular transverse cross-section it can be assumed that the section is in a plane state of deformation, with the normal stresses in the plane of the cross-section and σ_z parallel to the vertical axis of the member. Therefore, in this simplified model the increase in the bearing capacity of the member is due to the share of normal stress depending on the confinement lateral stresses. It is possible to further simplify the three dimensional model by assuming a plane model and considering, for the symmetry of the system, only one quarter of the transverse cross-section, as shown in Fig. 2. When lateral expansion occurs in the concrete member, the displacement along the diagonal direction corresponds to the lateral elongations along the two sides of the cross-section.

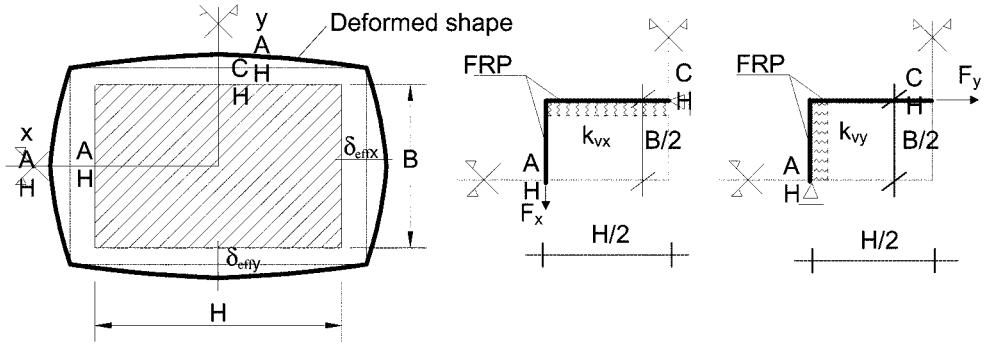

Fig. 2 Equivalent model

These elongations can be assumed to be produced by two elastic beams (FRP sheets) on unilateral springs (concrete) and connected at the corners of the cross-section.

The elastic beams on elastic springs are stiffened in flexure by including also the effect of axial forces in FRP, but because in wrapped rectangular cross-section the stresses in FRP are very low with respect to tensile strength of material and because very low thickness of reinforcing layers are utilised the above mentioned stiffness effect is negligible on the confinement pressures distribution. For practical purposes a further simplification consists in the model of elastic beams on elastic springs. The membrane effect can be taken into account by imposing (as it will shown in the following) that the displacement at the end of the beam (corner of cross-section) is equal to the elongation of the FRP package in the perpendicular direction.

For each beam, having length $B/2$ and $H/2$ respectively, springs distributed along the length of the beam itself, are considered. The springs have stiffness indicated with the symbol k_v, (k_{vx} and k_{vy} in x and y direction) acting in the direction perpendicular to the beam axis and simulating the interaction producing confinement pressures in the concrete core. The elastic analysis will be carried out by means of a simplified representation of the interaction phenomena allowing one to detect the parameters governing the problem; then an extension up to failure stage of the member will be given to determine the maximum bearing capacity.

Referring to the failure condition of concrete (peak load) it can be assumed that because of the shape of the transverse cross-section and of the low flexural stiffness of FRP package (with sharp corners and extended flat portion), the failure of concrete corresponds to the reaching of ultimate strain in tension of concrete core in the direction perpendicular to the axis of the compressed member, and in this condition ultimate stress in FRP is not reached.

This is in agreement with experimental observation made in Mirmiran *et al.* (1998) in which it was pointed out that if the ratio between the effective confinement pressure in concrete core, and the strength of unconfined concrete is very low (case of square and rectangular cross section with moderate number of reinforcing layers and small radius of corners) the maximum strength of confined concrete is lower than ultimate strength corresponding to failure of FRP (strain-softening behavior).

2.1 Confinement pressures

The two elastic beams simulating the FRP package have flexural stiffness proportional to the quantity $\frac{E_f \cdot t^3}{12}$, E_f being the modulus of elasticity and t the thickness of the FRP sheet. The elastic springs are considered acting each separately from the another and their stiffness takes the presence of the concrete core shell into account. This stiffness can be assumed to be proportional to the axial stiffness of the concrete shell in the plane of the cross-section. Its value for unit length is $k_v = \frac{2 \cdot E_c}{L \cdot (1-2 \cdot \nu_c)}$, E_c being the modulus of elasticity of concrete and L the side of the cross-section considered (being $L = H$ and $L = B$ in x and y direction for rectangular cross-section).

To determine the confinement pressures q it is assumed that the beam behaves as semi-infinite elastic beam on elastic spring subjected at the corner to a force F (F_x and F_y forces for rectangular cross-section). The equilibrium equation of the elastic beam of inertia I_f on elastic springs in a

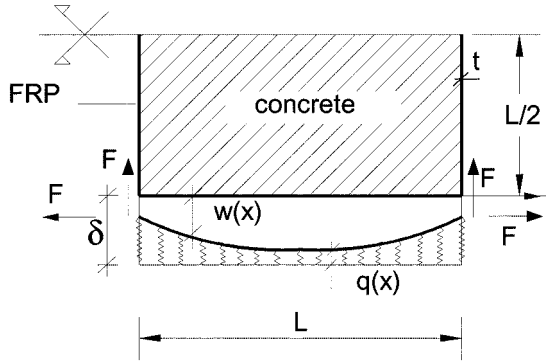

Fig. 3 Mechanical model

deformed configuration (see Fig. 3), in term of lateral displacements *w*, is governed by the following differential equation.

$$\frac{d^4 w}{dx^4} + \frac{k_v}{E_f \cdot I_f}(\delta - w) = 0 \tag{1}$$

being δ the lateral displacement of the unconfined concrete specimen.

By introducing $\beta = \sqrt[4]{\frac{3k_v}{t^3 \cdot E_f}}$ and by integrating the equilibrium equation imposing the boundary conditions $w(x = 0) = \frac{F \cdot L}{2 \cdot E_f \cdot t}$; $w''(x = 0) = 0$ results the following expressions of the displacement *w* and of the confinement pressure *q*:

$$w(x) = \left(\frac{F \cdot L}{2 \cdot E_f \cdot t} - \delta\right) \cdot e^{-\beta x} \cdot \cos(\beta x) + \delta \tag{2}$$

$$q(x) = k_v \cdot (\delta - w) = k_v \cdot \left(\delta - \frac{F \cdot L}{2 \cdot E_f \cdot t}\right) \cdot e^{-\beta x} \cdot \cos(\beta x) \tag{3}$$

And consequently the resultant of confining pressures:

$$R = \int_0^{L/2} q(x)dx = k_v \cdot \left(\delta - \frac{F \cdot L}{2 \cdot E_f \cdot t}\right)\frac{1}{2 \cdot \beta}\left[1 - e^{-\beta\frac{L}{2}} \cdot \left(\cos\frac{\beta \cdot L}{2} - \sin\frac{\beta \cdot L}{2}\right)\right] \tag{4}$$

To determine the axial forces in FRP the equilibrium between the resultant of confinement pressures in *x* and *y* direction and the axial forces in FRP is imposed.

With reference to Fig. 3 by imposing $R = F$ and neglecting the terms in brackets of Eq. (4), containing the exponential function, it results:

$$F = \frac{k_v \cdot \delta}{2 \cdot \beta} \cdot \frac{1}{\left(1 + \frac{k_v \cdot L}{4 \cdot E_f \cdot t \cdot \beta}\right)} \tag{5}$$

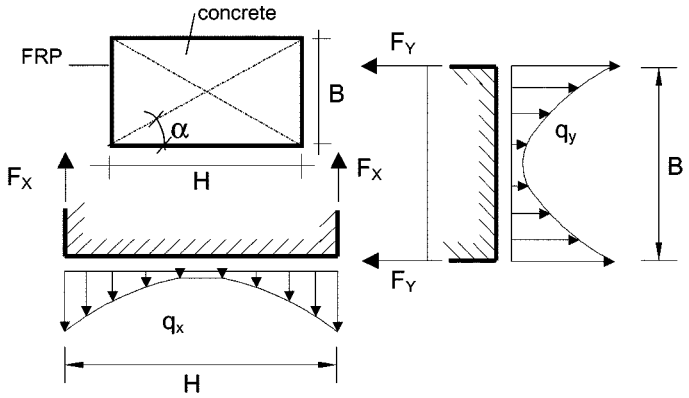

Fig. 4 Model for equilibrium of cross-section

In the case of rectangular cross-section F_x and F_y forces (see Fig. 4) arise relative to the confinement pressures in x and y direction.
By using Eq. (5) with $L = B$ or $L = H$ and introducing the k_{vx}, k_{vy} stiffness result:

$$F_x = \frac{k_{vx} \cdot \delta_x}{2 \cdot \beta} \cdot \frac{1}{\left(1 + \frac{k_{vx} \cdot H}{4 \cdot E_f \cdot t \cdot \beta_x}\right)} \tag{6}$$

$$F_y = \frac{k_{vy} \cdot \delta_y}{2 \cdot \beta_y} \cdot \frac{1}{\left(1 + \frac{k_{vy} \cdot B}{4 \cdot E_f \cdot t \cdot \beta_y}\right)} \tag{7}$$

$$\beta_x = \sqrt[4]{\frac{3k_{vx}}{t^3 \cdot E_f}}, \quad \beta_y = \sqrt[4]{\frac{3k_{vy}}{t^3 \cdot E_f}} \tag{8}$$

$$k_{vx} = \frac{2 \cdot E_c}{H \cdot (1 - 2 \cdot \nu_c)}, \quad k_{vy} = \frac{2 \cdot E_c}{B \cdot (1 - 2 \cdot \nu_c)} \tag{9}$$

Being $\delta_y = \delta_x/\tan(\alpha)$, with α the angle between the diagonal direction in rectangular cross-section and the longest side H (see Fig. 4).

2.2 Equivalent uniform lateral pressure

Results mentioned in the previous section have shown that confinement lateral pressures expressed by Eq. (3) are not uniform along the perimeter of the cross-section. In a simplified way, reduced uniform confining pressure can be utilised by means of a corrective coefficient k, better defined in the following. Similar approach, but of empirical nature, was that of Campione and Miraglia (2003) utilised for members with square cross-sections wrapped with FRP, and also in Ravzi and Saatchoglu (1999) for concrete members confined by transverse steel. In the latter the k coefficient was assumed equal to unity when the confinement pressure is near-uniform (as in the case of

closely spaced circular spirals) and variable with mechanical and geometrical parameters for non uniform pressures. In particular the k coefficient is less than one and is a function of tie spacing, length of the side of transverse cross-section and of spacing of laterally supported longitudinal reinforcements.

In the present paper the coefficient k is introduced as a stress reducing factor that in elastic stage can be derived by Eq. (5) as the ratio between the actual stress in fiber σ and the ultimate stress f_u:

$$k = \frac{1}{2 \cdot \beta} \cdot \frac{1}{t \cdot f_u} k_v \cdot \delta \cdot \frac{1}{\left(1 + \frac{k_v \cdot L}{4 \cdot E_f \cdot t \cdot \beta}\right)} \tag{10}$$

The cases of shaper corners, as shown by elastic analyses carried out by using finite element analyses, determine very low confinement pressures localised across the corners of the cross section and for this reason in the following failure criteria determining maximum strength will be assumed, as already mentioned, the condition in which concrete reached ultimate strain in tension in direction perpendicular to loading axis.

During the loading process the Poisson coefficient ν_c is variable with the axial strain ε_f. Moreover, to determine the maximum stress of confined members with cross-section having sharp corners or small radius of corners, good fitting with the experimental results can be obtained by assuming a ν_c value of 0.35. Also the secant modulus of elasticity is variable with the increasing in axial strain. At rupture it is reasonable to assume the modulus of elasticity equal to 2/3 E_c to give the best fitting with experimental results. Similar value was also assumed for the determination of maximum strength by Mander *et al.* (1988).

Based of this approach, the k coefficient at rupture can be obtained by Eq. (10) introducing the average strain in tension of concrete $\varepsilon_{ct} = 2\ \delta/L$ that was assumed equal to $\varepsilon_{ctu} = \nu_c\ (\varepsilon_c)$ with ν_c = 0.35 and ε_c = 0.004. The value of 0.004 of maximum axial strain, assumed by Mander *et al.* (1988) for concrete cover, is here assumed as a values of axial strain associated with the lateral strain reached in correspondence of the maximum strength of confined core. This value is justified because in the middle part of the flat portion of cross-section the confinement effect is negligible due to the low flexural stiffness of FRP package.

Moreover, by means of Eq. (10) introducing the average ultimate confining pressure $f_l = 2t\ f_u/L$ the k coefficient results:

$$k = \frac{2 \cdot \varepsilon_{ct} \cdot k_v \cdot E_f \cdot t}{f_l(4 \cdot E_f \cdot t \cdot \beta + k_v \cdot L)} \tag{11}$$

The f_u value above mentioned is the tensile strength given by the manufacturer of the FRP sheet. As suggested in Spoelstra and Monti (1999) for wrapped members with circular cross-section, this value is not possible to reach because of: - non perfect adhesion of reinforcing package; - loading of the fibers in their perpendicular direction; - delamitation phenomena of multilayer; etc. In the cases here presented, referred to section with sharp corners, a further penalization derives from the stress-concentration at corners and, for this reason at concrete peak load, the stress in FRP is only a few percentage of its tensile strength.

Eq. (11) shows that effectively confinement pressure, expressed as a percentage of ultimate uniform confining pressure, depends not only on the characteristics of fiber (modulus of elasticity and axial stiffness related to t), but also on the characteristics of the concrete core.

Similar conclusions, but of empirical nature, are also given in Chaallal *et al.* (2003) in which was mentioned that the gain in strength of concrete depends not only on the number of FRP layer, but also on the concrete properties. More accurate results can be obtained (see next section) considering the variation of the ν_c coefficient with the axial strain of confined concrete specimens and determining numerically the k coefficient at rupture when concrete reaches maximum strength.

In the case of rectangular cross-section the variation of transverse strains are not the same in long and short side of the members and two different Poisson's ratios (ν_x, ν_y) should be adopted. For simplicity of calculation and because no too slender cross-section are analysed only one Poisson ratio value was assumed in x and y direction.

Two different k factors have to be utilised having the following expressions:

$$k_x = \frac{2 \cdot \varepsilon_{ct} \cdot k_{vx} \cdot E_f \cdot t}{f_{lx}(4 \cdot E_f \cdot t \cdot \beta_x + k_{vx} \cdot H)} \tag{12}$$

$$k_y = \frac{2 \cdot \varepsilon_{ct} \cdot k_{vy} \cdot E_f \cdot t}{\tan(\alpha) \cdot f_{ly}(4 \cdot E_f \cdot t \cdot \beta_y + k_{vy} \cdot B)} \tag{13}$$

being $f_{lx} = 2t\, f_u/H$ and $f_{ly} = 2t\, f_u/B$.

In this case ultimate strain was assumed those reached perpendicularly to the longest side H; instead along the other side of length B the strain is equal to $\varepsilon_{ct} \tan \alpha$.

2.3 Local reinforcements with single FRP strips at the corners and smoothing of round corners

In this section some considerations on the interaction phenomena between concrete core and FRP wraps in the case of local reinforcements at the corners with single strips of FRP and in the case of smoothing of sharp corners with round fillets will be given.

The cases examined are shown schematically in Fig. 5. In particular the case of single strips at the corners was object of experimental research in Campione *et al.* (2003). In that investigation was shown that if single strips are applied at the corners of square or rectangular cross-section (with fiber orientation perpendicular at the axis of the compressed member) and applied before the wrapping with continuous layer, over strength at the corners develops.

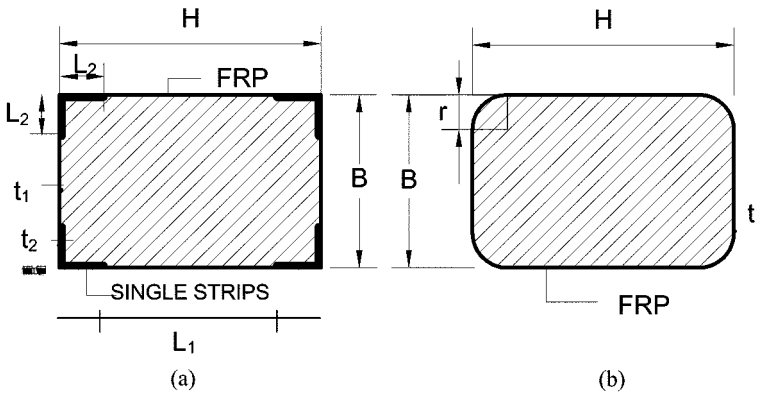

Fig. 5 Local reinforcing at the corners

Failure of fibers occurs along the flat part of the section rather then at the corner and increasing in the bearing capacity and in the ductility occur. This reinforcing technique is an alternative technique to the smoothing of sharp corners with adequate radii.

Fig. 5(a) refers also to a concrete member wrapped with FRP layers having t_2 thickness and L_2 length at the corners and t_1 thickness in the other part with length L_1 (respectively $B - 2\ L_2$ and $H - 2\ L_2$). In this case it is reasonable to assume that confinement pressure is determined as in the previous section considering the axial stiffness of a beam with two different transverse cross-section.

In this case Eq. (1) should be satisfied by imposing that $w(x = 0) = \frac{F}{2 \cdot E_f} \cdot \left(\frac{L_1}{t_1} + \frac{2 \cdot L_2}{t_2}\right)$; $w''(x = 0) = 0$ and being β referred to the beam of thickness t_2.

The deflection of the beam is expressed by:

$$w(x) = \left[\frac{F}{2 \cdot E_f} \cdot \left(\frac{L_1}{t_1} + \frac{2 \cdot L_2}{t_2}\right) - \delta\right] \cdot e^{-\beta x} \cdot \cos(\beta x) + \delta \tag{14}$$

consequently the confinement pressure and the axial force on FRP result:

$$q(x) = k_v \cdot \left(\delta - \frac{F}{2 \cdot E_f} \cdot \left(\frac{L_1}{t_1} + \frac{L_2}{t_2}\right)\right) \cdot e^{-\beta x} \cdot \cos(\beta x) \tag{15}$$

$$F = \frac{k_v \cdot \delta}{2 \cdot \beta} \cdot \frac{1}{\left[1 + \frac{k_v}{2 \cdot E_f \cdot \beta} \cdot \left(\frac{L_1}{t_1} + \frac{2 \cdot L_2}{t_2}\right)\right]} \tag{16}$$

In the case of smoothing of the corner with round fillets (see Fig 5b) it is possible to approach the problem in a similar manner as previously made for the section with sharp corners.

In particular with reference to a quarter of a circular cross-section (this is also the case of circular cross-section of radius R) it is possible to obtain the axial force in FRP with the variation in the δ displacement. By considering that the effective displacement w is equal to:

$$w = \delta - \frac{F}{E_f \cdot t} \tag{17}$$

and by considering that w is related to the internal confinement pressure by means of the axial stiffness of the cylinder $k_r = \frac{E_c}{R \cdot (1 - 2 \cdot \nu_c)}$ and considering also the equilibrium of the transverse cross-section related to the axial force F, it is possible to obtain the condition:

$$w = \frac{F}{R} \cdot \frac{R \cdot (1 - 2 \cdot \nu_c)}{E_c} \tag{18}$$

By using Eq. (17) and Eq. (18) it results:

$$F = \frac{\delta}{\frac{1}{E_f \cdot t} + \frac{1 - 2 \cdot \nu_c}{E_c}} \tag{19}$$

In the case of square section with round corners of radius r (with reference to the symbols of Fig. 5) an elastic beam of length $L/2 - r$ was considered connected to the perpendicular legs by means of a quarter of cylinder having axial stiffness k_r, while the stiffness of concrete core is k_v.

The Eq. (1) referred to the beam of length $L/2 - r$ should be integrated by imposing the boundary conditions:

$$w(x = 0) = F \cdot \left[\frac{1}{E_f \cdot t} \cdot \left(\frac{L}{2} - r + \frac{\pi \cdot r}{2}\right) + \frac{(1 - 2 \cdot \nu_c)}{E_c}\right] \tag{20}$$

$w''(x = 0) = 0$

Eq. (20) takes into account that the displacement at the tip of the beam is due also to the elongation of FRP along the round fillets and to the radial shortening of concrete cylinder having radius r. To determine the axial forces in FRP the equilibrium between the resultant of confinement pressures (in the beam of length $L/2 - r$ plus the contribution due to the circular shell) and the force F was imposed resulting:

$$F = \frac{\frac{k_v}{2 \cdot \beta} \cdot \left\{\left[1 - e^{-\beta \cdot \left(\frac{L}{2} - r\right)} \cdot \left(\cos\beta \cdot \left(\frac{L}{2} - r\right) - \sin\beta \cdot \left(\frac{L}{2} - r\right)\right)\right]\right\} \cdot \delta}{1 + \left[\frac{1}{E_f \cdot t} \cdot \left(\frac{L}{2} - r + \frac{\pi \cdot r}{2}\right) + \frac{1 - 2 \cdot \nu_c}{E_c}\right]\left\{\frac{k_v}{2 \cdot \beta} \cdot \left[1 - e^{-\beta \cdot \left(\frac{L}{2} - r\right)} \cdot \left(\cos\beta \cdot \left(\frac{L}{2} - r\right) - \sin\beta \cdot \left(\frac{L}{2} - r\right)\right)\right]\right\}} \tag{21}$$

As made for square cross-section a k coefficient can be derived from Eq. (21) by dividing F for t and f_u and introducing the average strain in tension ε_{ct}, but expression obtained which considers also the case of sharp and round corners is quite complex. Eq. (21) can also be extended to the case of rectangular cross-section.

For design purpose is appears more appropriate to assume that the presence of round fillets reduces stress-concentration in a linear manner as made in Wang and Restrepo (2001). By assuming that a linear variation of stresses in FRP with the radius of corners occurs, the following expressions can be utilised:

$$f_{rx} = \varepsilon_{fd} \cdot E_f \cdot \left[(1 - k_x) \cdot \frac{2 \cdot r}{H} + k_x\right] \tag{22}$$

$$f_{ry} = \varepsilon_{fd} \cdot E_f \cdot \left[(1 - k_y) \cdot \frac{2 \cdot r}{B} + k_y\right] \tag{23}$$

Eqs. (22, 23) form the limits of circular cross-section ($B = H = 2r$) and of square or rectangular cross-section by means of the reducing factor k_x, k_y. Results obtained by using Eq. (21) are in agreement with those obtained by Eqs. (22, 23).

Expressions here given confirm results obtained experimentally by Yang *et al.* (2001). They have shown that the stress variation in the fiber can be assumed linearly variable with the radius r of the corner for a moderate reinforcement level of FRP, while, when the number of plies increases, non-linear behavior is observed as can be obtained by Eq. (21).

The ε_{fd} value is the maximum strain reached in circular member wrapped with FRP at rupture of concrete core. Analytical (Spoelstra and Monti 1999) and experimental research (Mirmiran *et al.*

1998) have shown that ε_{fd} strain is lower than ultimate strain and in general is between 0.004 and 0.008. It is interesting to observe that the model proposed takes into account of the round fillets and also by means of k_x, k_y factors take into account of the geometric parameter, and of the concrete and FRP mechanical properties.

3. Maximum strength of FRP wrapped columns

As already observed in the previous sections, concrete confined by FRP wraps develops passive lateral pressure as it expands under axial compression, creating a multiaxial state of stress. The strength of concrete with non-linear and non homogeneous material characteristics under multiaxial state of stress may be difficult to establish theoretically. Recent analytical approaches, based on plasticity (Karabinis and Rousakis 2002), or fracture mechanics (Caner and Bazant 2002), were proposed to predict maximum strength increases and they fit very well experimental results. These models are often difficult to utilise and to calibrate. Empirical or semi-empirical approaches (e.g., Maalej *et al.* 2003) are utilised to give simple expressions of common use, calibrated on the basis of experimental data. Based on the latter approach the maximum compressive strength $f_{cc}^{'}$ and the maximum axial strain ε_{cc} can be assumed, as made originally in Richard *et al.* (1929), for concrete cylinders confined by uniform pressures, equal to:

$$f'_{cc} = f'_c + k_1 \cdot f'_1 \tag{24}$$

$$\varepsilon_{cc} = \varepsilon_0 \cdot \left(1 + k_2 \frac{k_1 \cdot k_e \cdot f_1}{f'_c}\right) \tag{25}$$

k_1, k_2 being proportionality coefficients generally assumed in accordance with experimental data (depending on the internal angle of friction of concrete core at rupture), f_c' and ε_0 the cylindrical compressive strength and the corresponding strain of unconfined concrete. Analytical values for maximum strength will be obtained in the following by adopting $k_1 = 4.1$ and $k_2 = 5$, as suggested in Mander *et al.* (1988), and also as made for wrapped members by Lam and Teng (2002).

Many analytical studies have also proposed, non linear expressions, correlating k_1 value with effective confining pressures and with the strength of unconfined concrete (e.g., Toutanji 1999).

In Eqs. (24, 25) the effective confinement pressure f_l' can be related, as made in Mander *et al.* (1988) for confinement induced by steel stirrups, to the confinement pressure f_l induced by FRP devices and to the effectiveness coefficients k_e, such as $f_l' = k_e \times f_l$. Both k_e and f_l depend on the arrangement and mechanical characteristics of reinforcing jackets and also on the shape of the transverse cross-section of the reinforced members as observed in the previous sections. In the following expressions of k_e and f_l will be given. Effective lateral pressure is determined following the suggestions of the previous chapter. No size effect, that reduces maximum strength with the size increasing (Theriault *et al.* 2001), is considered in the prediction of maximum strength.

3.1 Effectiveness coefficient k_e

For the calculus of k_e it can be assumed, as shown in Fig. 6, that in the case of a circular cross-section the full area of concrete enclosed in FRP wraps is effectively confined, while in a square or

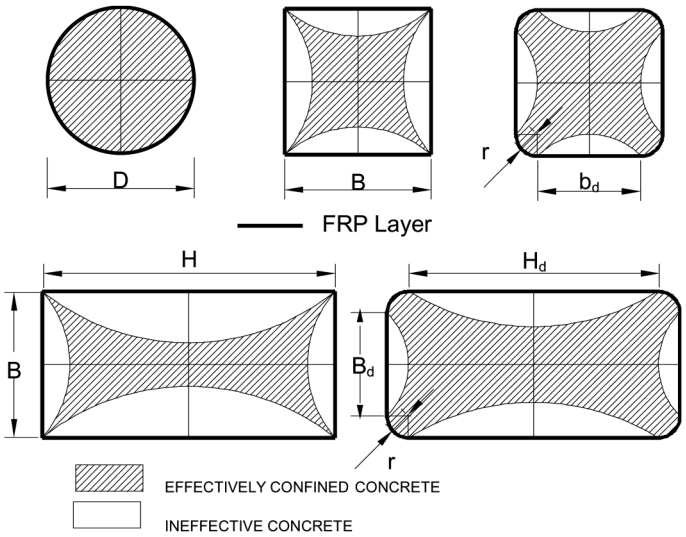

Fig. 6 Effective confined area in transverse cross-section of FRP wrapped members

rectangular cross-section a reduction in the gross area occurs, due to the arching action.

In the latter case, due to the sharp edges, a reduction in plan of concrete core was assumed, as in members reinforced with steel stirrups. No further reduction of effectively concrete core along the height of the specimens was assumed, because the application of reinforcing layer is continuous along the height of the concrete member. For rectangular cross-section the ineffectively confined areas can be assumed enclosed by second-degree parabolas with an initial tangent slope of 45° (as suggested in Mander *et al.* 1988), while in the case of rectangular section with round fillets at the corners an additional confined concrete area at rupture was assumed as shown in Fig. 6. The confinement effectiveness coefficient k_e is evaluated for rectangular cross-section with rounded corners (CEB-FIP 2001) as:

$$k_e = 1 - \frac{H_d^2 + B_d^2}{3 \cdot \left[H \cdot B - 4 \cdot \left(r^2 - \frac{\pi \cdot r^2}{4} \right) \right]} \tag{26}$$

Fig. 7 shows the variation in k_e with an increase in the ratio H/B for a given corner radius (r/B). It is interesting to note that for a rectangular cross-section ($r/B = 0$), if the ratio H/B is more then 2, k_e value is very low and reduced confinement effect is expected.

Better performances are obtained for $r/B = 0.06$ and 0.1, corresponding to r between 15 and 25 mm, forming the range of minimum values suggested by CEB-FIP (2001). From considerations given it emerges that if corners of square or rectangular cross-sections are rounded the effectively confined concrete core increases. But, if the rectangular cross-section has a ratio between the two sides higher than 2, no confinement effects are expected independently of the number of plies of FRP utilised.

In these cases it appears more appropriate to modify the shape of the rectangular cross-section by adding new material before wrapping the section with the FPR layer.

As suggested also in CEB-FIP (2001), the best section shape to transform the rectangular cross-

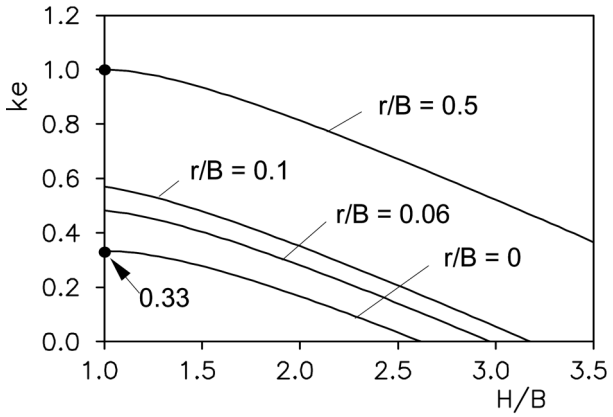

Fig. 7 Variation in effectiveness coefficient k_e with *H/B*

section is the circular or oval shape. If an elliptical cross-section is adopted the choice of the ratio between the length of the two axis of elliptical cross-section is related to the fact that ellipse has to fit the rectangular cross-section and it should also give the highest k_e value.

3.2 Effective confinement pressure and effective stresses in FRP

To determine the lateral confinement pressure due to FRP wraps it is possible to refer to the equilibrium of the cross-section, considered as if it is a rigid body shown in Fig. 8.

In this case the stresses along the fiber can be assumed equal to:

$$f_{lx} = \frac{2 \cdot F_x}{H} \quad \text{in } x \text{ direction} \tag{27}$$

$$f_{ly} = \frac{2 \cdot F_y}{B} \quad \text{in } y \text{ direction} \tag{28}$$

In the case of rectangular cross-section with round corners stresses along the fiber can be assumed equal to f_{rx} and f_{ry} obtained using Eqs. (22, 23) in a simplified way, and being F_{rx} and F_{ry} deduced in the previous section.

Because the columns have different confining pressures in the two orthogonal directions, if Eq. (24) is utilised to predict maximum strength, an equivalent confinement pressure f_l can be obtained as in

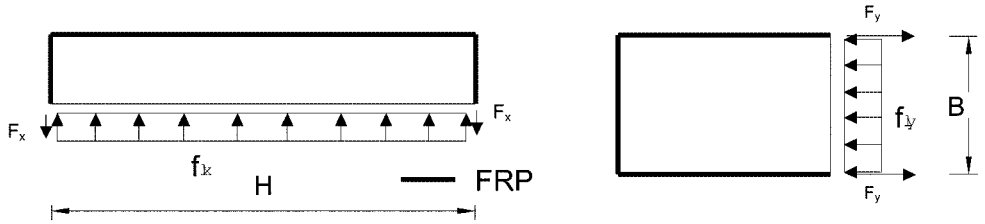

Fig. 8 Confinement pressure in rectangular cross-section wrapped with FRP

Cusson and Paultre (1995), by assuming that the different confinement pressures f_{lx} and f_{ly} might be considered as:

$$f_l = \frac{f_{lx} \cdot H + f_{ly} \cdot B}{B + H} \tag{29}$$

4. Ultimate strain capacities of wrapped member

Several analytical expressions are given in the literature for the calculus of the maximum strain of compressed members wrapped with FRP. Some of these expressions are based on the determination of the maximum longitudinal strain corresponding to the volumetric deformation of concrete core reached when the confinement effect is maximum (Spoelstra and Monti 1999) and ultimate strain occur in FRP in tension; other expressions are of a semi-empirical nature, such as that suggested by Seible *et al.* (1997). The latter, also mentioned in CEB-FIB (2001) has the following expression for circular cross-sections:

$$\varepsilon_{cu} = 0.004 + \frac{2.5 \cdot \rho_f \cdot f_j \cdot \varepsilon_{ju}}{f'_{cc}} \tag{30}$$

ρ_f being the geometrical percentage of FRP area referred to the gross section of concrete members having circular cross-section (with $\rho_f = 4t/D$, and D external diameter), f_j and ε_{ju} the effective stress, and strain in FRP and f'_{cc} the strength of confined concrete.

Good and conservative results are also obtained by using the formula recently given by Campione and Miraglia (2003), valid for the case of a square cross-section with round corners in which an approximate expression for ε_{cu} was given valid when strain-hardening behavior of concrete was observed. In the cases in which strain-softening behavior is observed rupture of FRP occur in the softening branch when concrete core have already reached ultimate stress.

In this case, with reference to the symbol of Fig. 9, it is possible to determine the ε_{cu} value, by numerical approach, knowing the complete stress-strain curve of confined concrete.

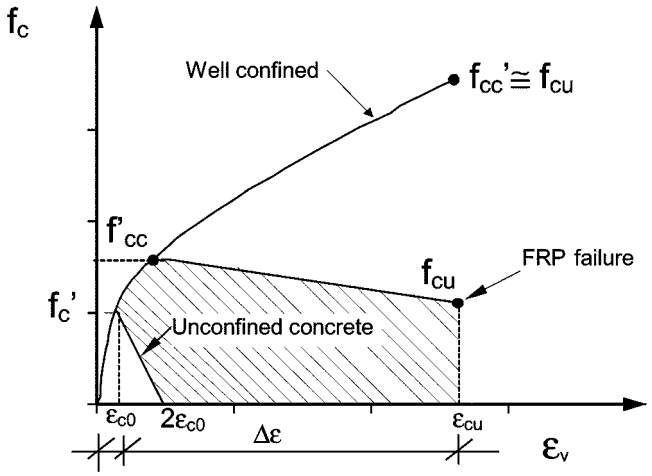

Fig. 9 Stress-strain model in compression for calculation of ultimate concrete strain

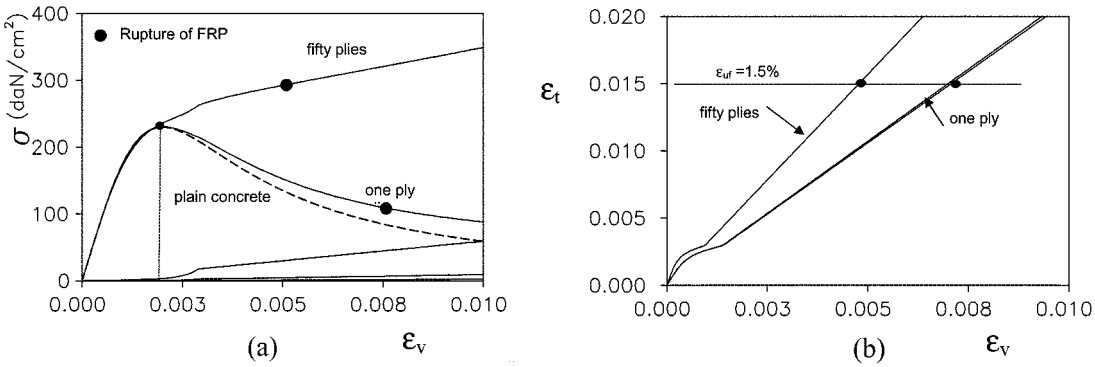

Fig. 10 Stress-strain relationship and axial strain in concrete with variation of strain in FRP

The stress-strain relationship here utilised is that mentioned in Mander *et al.* (1988) in the following form:

$$\sigma_c = \frac{f_{cc} \cdot \dfrac{\varepsilon_c}{\varepsilon_{cc}} \cdot \gamma}{\gamma - 1 + \left(\dfrac{\varepsilon_c}{\varepsilon_{cc}}\right)^{\gamma}} \tag{31}$$

in which $\gamma = \dfrac{E_c}{E_c - \dfrac{f_{cc}}{\varepsilon_{cc}}}$

To determine the ultimate strain, as shown in Fig. 10, the following procedure is utilised. For simplicity the case of square cross-section was considered.

A initial value of average axial strain ε_c was assumed with the first value zero. Assuming a the following variation law of the v_c coefficient with the axial strain (this is that given in Elwi and Murray 1979) the lateral strain measured in the middle of the side was obtained as $\varepsilon_t = v_c\, \varepsilon_c$.

The above mentioned v_c coefficient is:

$$v = v_0 \cdot \left[1 + 1.38 \cdot \frac{\varepsilon}{\varepsilon_{cu}} - 5.36\left(\frac{\varepsilon}{\varepsilon_{cu}}\right)^2 + 8.59 \cdot \left(\frac{\varepsilon}{\varepsilon_{cu}}\right)^3\right] \tag{32}$$

being v_0 the elastic Poisson ratio assumed equal to 0.20, $\varepsilon_{cu} = 2\varepsilon_{c0}$ the ultimate strain of unconfined concrete.

Therefore the displacement δ is know because $\varepsilon_t = 2\delta/L$ and, by using the proposed model of the previous sections, the forces in FRP are determined and so on the equivalent average confinement pressure variable for each step. By using Eq. (21) and Eq. (24) the stress in concrete core and the maximum strength were obtained for each strain increases. Repeating this procedure for all possible values of axial strain complete stress-strain curve is plotted. Moreover, the axial strain in FRP with the variation in axial strain of concrete core is known.

By imposing failure of FRP, the value of axial shortening is determined. This is the value of shortening in concrete core corresponding to failure of FRP in tension.

In Fig. 10 is plotted an example relative to the proposed procedure for a square cross-section wrapped with different number of carbon fiber reinforcing layer.

The cases examined in the graph refer to members having square cross-section of sides 150 mm with concrete having cylindrical strength of 22 MPa and wrapped with thin layer of high-strength, high-modulus carbon fiber having 0.165 mm thickness for each layer.

Fig. 10(a) gives stress-strain curves, while Fig. 10(b) gives lateral strain in FRP versus axial shortening. It is interesting to observe that in the case of moderate reinforcing confinement ultimate strain is reached in concrete core in the softening branch, while if very high confinement pressure is applied (it is only a theoretical case for sharp corners should be used more than fifty layers) maximum strength and ultimate strength are quite the same.

It is interesting to observe that the confinement effect is not proportional to the number of plies because of the combination of concrete and FRP package characteristics and, moreover, the confinement effect is negligible for section with sharp corners and with thin layers of reinforcing package.

Analyses carried out also confirm that ultimate strain of 0.004 with a value of 0.35 for Poisson coefficient gives good prediction of stresses in FRP at rupture of concrete core and they are reliable as design values as assumed in the previous sections.

5. Experimental validation and comparison with analytical results

In the present section are briefly summarised experimental results relative to previous investigation carried out by the authors (Campione *et al.* 2003). The experimental research carried out concerned prismatic specimens having square and rectangular cross-sections and subjected to concentric compressive loads. Prisms with rectangular transverse cross-section have dimensions 150×150 and 150×300 mm with height $h = 450$ mm. Some of the specimens are made of plain concrete, others were reinforced by wrapping them externally with unidirectional carbon fiber reinforced plastic sheets glued with epoxy resin. The concrete has compressive cylindrical strength at 28 days (measured on 100×200 mm specimen) of $f_c' \approx 13$ MPa. Although the low strength class is rather unrealistic for new constructions, the choice of a very low concrete strength aims to show the effectiveness of the CFRP wrapping technique on the behavior in compression of a concrete member having low bearing capacity, such as it is common to have in several existing reinforced concrete structures. Similar concrete strength was utilised in experimental research on effects of confinement produced by FRP in Wang and Restrepo (2001). Fig. 11 shows concrete specimens having square cross-section and wrapped with CFRP and with over-lap length of 100 mm. Some specimens were wrapped with one, two and three layers of CFRP applied over almost all their length. The wrapping of the end portions of the specimens was avoided to avoid loading of CFRP in the longitudinal direction. High strength, high modulus carbon fiber sheets, type MBrace C1-30, were utilised.

The overlap length was chosen by the authors after previous studies (Campione *et al.* 2001, Ilki and Kumbasar 2002) to avoid premature debonding failure of fibers. Additional local reinforcements constituted by CFRP strips were applied at the corners of the specimens with the same height and orientation as the continuous layer and with over-lap 50 mm for each side, before the application of continuous layer (Fig. 11). After bending of CFRP layers there is a minimum radius of 3 mm at the corners, due to the manufacturing process.

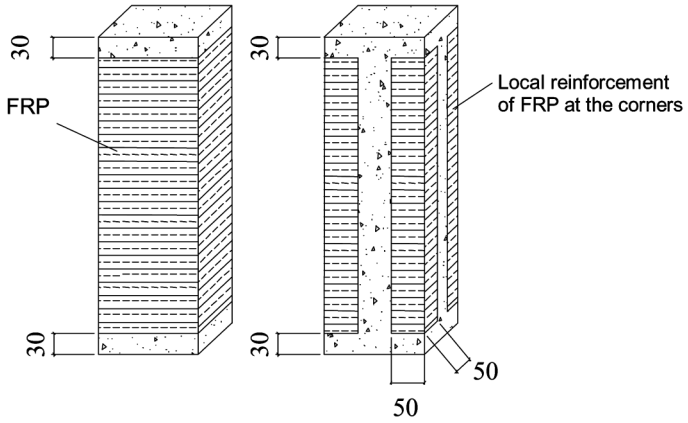

Fig. 11 Details of local reinforcements in CFRP at the corners

Fig. 12 shows stress-strain curves for prismatic specimens having side 150 mm and height 450 mm. The cases of concrete specimens wrapped with one or two layers of CFRP sheets are examined, as well as the cases of one, two or three layers of CFRP in the presence of local reinforcements constituted by CFRP strips at the corners.

From the trend of the curves it emerges that all specimens behave elastically in the first branch of the response and the initial stiffness is not influenced by the presence of CFRP. Therefore, when the maximum strength of plain concrete is reached, the presence of CFRP sheets produces an increase in maximum strength and strain values. When the maximum compressive strength is reached, a softening branch occurs and the progressive rupture of concrete core governs the failure, until the ultimate strain is reached in CFRP and rupture in tension of the reinforcing sheet occurs.

The experimental results obtained show that the use of two layers of CFRP is equivalent, in terms of increase in maximum strength, to the use of one layer and of local reinforcements at the corners. The latter technique allows a reduction in the quantities of material required and it is cheaper than the smoothing of sharp corners (which is not always possible). Both for square and rectangular cross-sections failure of CFRP in tension was observed. In particular brittle failure was observed at

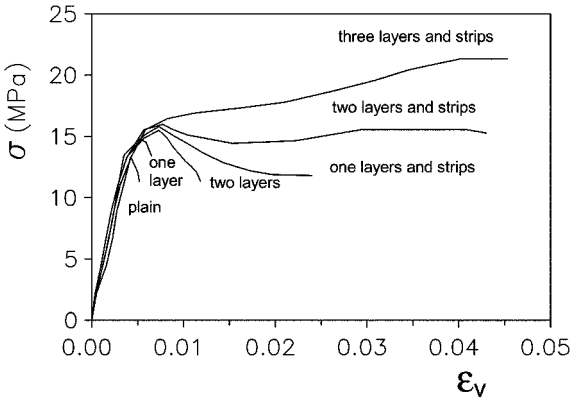

Fig. 12 Axial load-shortening curves for wrapped 150 × 150 × 450 mm specimens

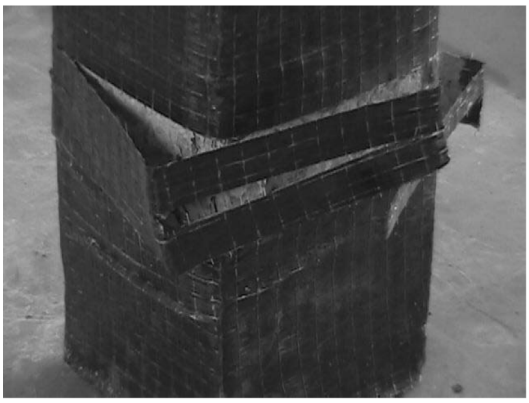

Fig. 13 Failure mode of CFRP wrapped specimens

the corners for specimens wrapped with CFRP (Fig. 13) and without local reinforcements and a more progressive mode of failure along the sides of the specimens locally reinforced at the corners was observed.

Unfortunately very few data exist in the literature on the technique of local reinforcement at the corners with single strips of FRP, and more extensive experimental research should be developed to give more general conclusions.

In Table 1 are given geometrical properties of transverse cross-section and mechanical characteristics of concrete and FRP reinforcing layers for several cases given in the literature (Rochette and Labossiére 2000, Wang and Restrepo 2001, Shehata *et al.* 2002, Campione *et al.* 2003, Ignatowski and Kaminska 2003).

The tests mentioned refer to square and rectangular cross-sections rounded at the corners with different radius of corners r and reinforced with unidirectional carbon or glass FRP wraps placed with the fibers perpendicular to the axis of the compressed members. All test mentioned refer to strain-softening behavior.

Table 1 Geometrical and mechanical characteristics of wrapped specimens

Ref.	Dimensions (mm)	r (mm)	f_c' (MPa)	FRP type	f_u (MPa)	ε_u (%)	E_f (GPa)	t (mm)	n^o layers
Rochette and Labossière (2000)									
1	152 × 203	25	42.0	Carbon	1265	1.50	82.7	0.90	3
2	“	38	42.0	“	“	“	“	0.90	3
3	“	5	43.9	“	“	“	“	1.20	4
4	“	25	43.9		“	“	“	1.50	5
Shehata *et al.* (2002)									
5	94 × 188	10	25	Carbon	3550	1.50	235	0.165	1
6	“	“	25	“	“	“	“	0.330	2
Wang and Restrepo (2001)									
7	300 × 450	30	13.5	Glass	375	2.0	20.5	2.54	2
8	“	“	“	“	“	“	“	7.16	6
Campione *et al.* (2003)*									
9	150 × 150	3	13.0	Carbon	3430	1.5	230	0.165	1
10	“	“	“	“	“	“	“	0.330	2
11	“	“3	“	“	“	“	“	0.495	3
Ignatowski and Kaminska (2003)									
12	100 × 100	10	32.3	Carbon	3500	1.5	230	0.260	2
13	105 × 200	“	“	“	“	“	“	0.130	1
14	“	“	“	“	“	“	“	0.260	2
Mirmiran *et al.* (1998)									
15	152 ×152	6.35	40.6	Glass	2186	1.5	69.64	1.45	6
16	“	“	“	“	“	“		2.21	10
17	“	“	“	“	“	“		2.97	14

*specimens reinforced also with single strips at corners

Table 2 Compressive strength and ultimate strains values for the concrete wrapped columns

Ref.	Experimental		Analytical					
	f'_{cc}/f'_c	$\varepsilon_{cu}/\varepsilon_{co}$	k_{rx}	k_{ry}	k_e	f_l/f'_c	f'_{cc}/f'_c	$\varepsilon_{cu}/\varepsilon_{co}$
Rochette and Labossière (2000)								
1	1.00	3.95	0.28	0.35	0.63	0.050	1.11	1.95
2	1.04	4.25	0.40	0.51	0.76	0.096	1.19	1.80
3	1.01	4.65	0.10	0.10	0.38	0.013	1.03	2.40
4	1.19	4.90	0.28	0.35	0.63	0.088	1.17	2.00
Shehata *et al.* (2002)								
5	1.11	/	0.14	0.23	0.36	0.02	1.04	/
6	1.34	/	0.13	0.22	0.36	0.04	1.08	/
Wang and Restrepo (2001)								
7	1.10	3.45	0.18	0.23	0.48	0.03	1.06	4.50
8	1.40	4.00	0.17	0.22	0.48	0.09	1.17	5.00
Campione *et al.* (2003)								
9	1.17	/	011	0.11	0.43	0.02	1.05	/
10	1.38	/	0.10	0.10	0.43	0.05	1.10	/
11	1.41	/	0.10	0.10	0.43	0.07	1.15	/
Ignatowski and Kaminska (2003)								
12	1.35	3.44	0.23	0.23	0.57	0.07	1.14	1.20
13	1.16	1.36	0.14	0.20	0.37	0.01	1.04	1.75
14	1.26	2.72	0.13	0.20	0.37	0.02	1.07	1.90
Mirmiran *et al.* (1998)								
15	1.07	4.33	0.11	0.11	0.44	0.04	1.08	5.00
16	1.13	4.16	0.10	0.10	0.44	0.06	1.13	4.50
17	1.14	5.16	0.10	0.10	0.44	0.08	1.17	4.95

In Table 2 are shown increases in maximum strength and strain values referred to the previously mentioned data of Table 1. The comparison shows acceptable agreement between analytical and experimental results. A correlation factor between analytical and experimental values results equal to 0.93 for strength prevision and equal to 0.82 for strain prediction.

6. Conclusions

This study presents a theoretical model for prediction the maximum strength and strain capacities of short compressed column externally wrapped with FRP sheets. Members with rectangular cross-sections and sharp or round corners were analysed.

Elastic analyses carried out to study the interaction phenomena between concrete core and FRP layers for section with sharp corners highlight that:

- confinement pressure distributions are not uniform along the sides of the transverse cross-section and maximum values occur at the corners, consequently very low average confining pressure because of the low flexural stiffness of reinforcing package are developed; moreover interaction phenomena is governed by the stiffness of concrete core in the transverse direction (modulus of elasticity, Poisson ratio, dimension of concrete core), and by the axial stiffness of reinforcing package (thickness, modulus of elasticity);
- at peak load the effective distribution of confinement pressure can be replied considering a uniform value by means of a reduction factor;
- local reinforcements considered in the model constituted by single strips reduced the risk of local failure in FRP due to stress concentration, and they are a good alternative to the smoothing of sharp corners.

Ultimate strain values, corresponding to FRP failure in tension, were obtained by considering the effective stress in concrete core corresponding to failure in tension of FRP by means of a numerical approach. Finally, comparison between analytical and experimental results of the literature show acceptable agreement, and physical model explains quite in details the interaction phenomena between concrete core and FRP package.

References

Campione, G., Miraglia, N. and Scibilia, N. (2001), "Comportamento in compressione di elementi in calcestruzzo armato a sezione quadrata e circolare rinforzati con FRP", *Ingegneria Sismica*, **2**, 5-12 (only available in Italian).

Campione, G. and Miraglia, N. (2003), "Strength and strain capacities of concrete compression members reinforced with FRP", *Cement & Concrete Composites*, **25**(1), 31-41.

Campione, G., Miraglia, N. and Papia, M. (2003), "Influence of section shape and wrapping technique on the compressive behavior of concrete columns confined with CFRP sheets", *Proc. Int. Conf. Composites in Constructions*, Bruno *et al.* (eds.), 216-221.

Caner, F.C. and Bazant, Z.P. (2002), "Lateral confinement needed to suppress softening of concrete in compression", *J. Eng. Mech.*, ASCE, **128**(12), 1304-1313.

Chaallal, O., Hassen, M. and Shahawy, M. (2003), "Confinement model for axially loaded short rectangular columns strengthened with fiber-reinforced polymer wrapping", *ACI Struct. J.*, **100**(2), 215-221.

CEB-FIP Bulletin 14 (2001), "Externally bonded FRP reinforcement for RC structures".

Cusson, D. and Paultre, P. (1995), "Stress-strain model for confined high-strength concrete", *J. Struct. Engng.*, ASCE, **121**(3), 468-477.

Demers, M. and Neale, W.K. (1999), "Confinement of reinforced concrete columns with fibre-reinforced composite sheets - An experimental study", *Can. J. Civ. Eng.*, **26**, 226-241.

Elwi, A.A. and Murray, D.W. (1979), "A 3D hypoelastic concrete constitutive relationship", *J. Eng. Mech.*, ASCE, **105**, 623-641.

Karabinis, A.I. and Rousakis, T.C. (2002), "Concrete confined by FRP material: A plasticity approach", *Eng. Struct.*, **24**, 923-932.

Kiang, H.T. (2002), "Strength enhancement of rectangular reinforced concrete columns using fiber-reinforced polymer", *J. of Comp. for Constr.*, ASCE, **6**(3), 175-183.

Ilki, A. and Kumbasar, N. (2002), "Behavior of damaged and undamaged concrete strengthened by carbon fiber composite sheets", *Struct. Engrg. Mech.*, **13**(1), 75-90.

Ignatowski, P. and Kaminska, M.E. (2003), "Concrete confinement with CFRP composites" *Proc. Int. Conf. Composites in Constructions*, Bruno *et al.* (eds.), 361-366.

Lam, L. and Teng, J.G. (2002), "Strength models for fiber-reinforced plastic-confined concrete", *J. Struct. Eng.*, ASCE, **128(**5), 612-623.

La Tegola, A. and Manni, O. (1998), "Structural behavior of concrete elements confined with FRP", *Proc. of ECCM Conf.*, 323-330
Maalej, M., Tanwongsval, S. and Paramasivam, P. (2003), "Modelling of rectangular RC columns strengthened with FRP", *Cement & Concrete Composites*, **25**, 263-276.
Mander, J.B., Priestley, M.J.N. and Park, R. (1988), "Theoretical stress-strain model for confined concrete", *J. Struct. Engrg.*, ASCE, **114**(8), 1804-1826.
Mirmiran, A., Shahawy, M., Samaan, M., EL Echary, H., Mastrapa, J.C. and Pico, O. (1998), "Effect of column parameters on FRP-confined concrete", *J. of Comp. for Constr.*, ASCE, **2**(4), 175-185.
Moran, D.A. and Pantelides, C.P. (2002), "Stress-strain model for fiber-reinforced polymer-confined concrete", *J. of Comp. for Constr.*, ASCE, **6**(4), 233-240.
Purba, B.K. and Mufti, A.A. (1999), "Investigation of the behavior of circular concrete columns reinforced with carbon fiber reinforced polymer (CFRP) jackets", *Can. J. Civ. Eng*., **26**, 590-596.
Richart, F.E., Brandtzaeg, A. and Brown, R.L. (1929), "The failure of plain and spiral reinforced concrete in compression", *Engineering Experiment Station*, Bulletin N. 190, University of Illinois, Urbana, USA.
Rochette, P. and Labossière, P. (2000), "Axial testing of rectangular column models confined with composites", *J. of Comp. for Constr.*, ASCE, **4**(3), 129-136.
Ravzi, S. and Saatcioglu, M. (1999), "Confinement model for high-strength concrete", *J. of Struct. Engrg.*, ASCE, **125**(3), 261-289.
Saadatmanesh, H., Ehsani, R.M. and Jin, L. (1997), "Repair of earthquake-damaged RC columns with FRP wraps", ACI *Struct. J.*, **94**(2), 206-215.
Saafi, M., Toutanji, H.A. and Li, Z. (1999), "Behavior of concrete columns confined with fiber reinforced polymer tubes", ACI *Material J.*, **96**(4), 500-509.
Seible, F., Priesley, M.J.N., Hegemier, G.A. and Innamorato, D. (1997), "Seismic retrofit of R.C. columns with continuous carbon fiber jackets", *J. of Comp. for Const.*, ASCE, **1**(2), 52-62.
Shehata, I.A.E.M., Carneiro, L.A.V. and Shehata, L.C.D. (2002), "Strength of short concrete columns confined with CFRP sheets", *Materials and Structures*, **35**, 50-58.
Spoelstra, M.R. and Monti, G. (1999), "FRP-confined concrete model", *J. of Comp. for Constr.*, ASCE, **3**(3), 143-150.
Tan, K.H. (2002), "Strength enhancement of rectangular reinforced concrete columns using fiber-reinforced polymer", *J. of Comp. for Constr.*, ASCE, **6**(3), 175-183.
Thériault, M., Claude, S. and Neale, K.W. (2001), "Effect of size and slenderness ratio on the behavior of FRP-wrapped columns", *FRPRCS-5*, Thomas Telford, London, 765-771.
Toutanji, H.A. (1999), "Stress-strain characteristics of concrete columns externally confined with advanced fiber composite sheets", ACI *Material J.*, **96**(3), 397-404.
Teng, G.J. and Lam, L. (2002), "Compressive behavior of carbon fiber reinforced polymer-confined concrete in elliptical columns", *J. Struct. Engrg.*, ASCE, **128**(2), 1535-1543.
Yang, X., Nanni, A. and Chen, G. (2001), "Effect of corner radius on the performance of externally bonded FRP reinforcement", *Proc. of FRPRCS5*, Non-metallic reinforcement for concrete structures, Cambridge, UK, July, 16-18.
Wang, C.Y. and Restrepo, J.I. (2001), "Investigation on concentrically loaded reinforced concrete columns confined with glass fiber-reinforced polymer jackets", ACI *Struct. J.*, **98**(3), 377-385.

Notation

B : base of the rectangular cross-section
E_c : modulus of elasticity of concrete
E_f : modulus of elasticity of FRP
E_{csec} : secant modulus of elasticity of concrete at peak load
f_c' : compressive strength of unconfined concrete
f_{cc}' : compressive strength (peak stress) of confined concrete
f_l : lateral confining stress on concrete core from FRP transverse reinforcement

f_l' : effective lateral confining stress
f_{lx} : lateral confining stress acting on concrete in the x direction
f_{ly} : lateral confining stress acting on concrete in the y direction
f_{rx} : stress of FRP composite in x direction
f_{ry} : stress of FRP composite in y direction
f_u : ultimate strength of FRP wraps
F : force in FRP
F_x : force in FRP in x direction
F_y : force in FRP in y direction
H : height of the rectangular cross-section
h : length of the specimen
I_f : moment of inertia of FRP package
L : length of the side of concrete specimen
L_1 : length of FRP package of thickness t_1
L_2 : length of FRP package of thickness t_2
P : axial force in compression
r : corner radius of cross-section
t : thickness of FRP layer
t_1 : thickness of minor FRP layer
t_2 : thickness of major FRP layer
k_e : confinement effectiveness coefficient for FRP confined cross-section
k_v : equivalent stiffness of concrete shell
k_{vx} : equivalent stiffness of concrete shell in x direction
k_{vy} : equivalent stiffness of concrete shell in y direction
k : reduction factor of ultimate stress in FRP
k_x : reduction factor of ultimate stress in FRP in x direction
k_y : reduction factor of ultimate stress in FRP in y direction
k_1 : concrete strength enhancement coefficient
k_2 : concrete strain enhancement coefficient
W : effective lateral displacement of confined specimen
β : parameter describing the stiffness of FRP - concrete shell
ε_0 : nominal maximum axial strain of unconfined concrete
ε_1 : hampered lateral strain in concrete
ε_{eff} : effective lateral strain in concrete
ε_{ct} : ultimate strain of concrete in tension
ε_0 : axial strain at peak load of unconfined concrete
ε_{fd} : ultimate design strain of FRP
ε_{cu} : nominal ultimate strain of confined concrete corresponding to FRP failure
ε_v : axial strain in concrete
δ : lateral displacement of unconfined concrete specimen
δ_x : lateral displacement of unconfined concrete specimen in x direction
δ_y : lateral displacement of unconfined concrete specimen in y direction
δ_v : axial shortening of specimens
ν_c : Poisson ratio of concrete
σ : nominal axial stress
σ_x : stress in x direction
σ_y : stress in y direction
σ_z : stress in z direction
ρ_f : transverse FRP reinforcement ratio
γ : shape parameter of stress-strain curves